



HAL
open science

Thermal characterization of biofouling around a dynamic submarine electrical cable

Ziad Maksassi, Bertrand Garnier, Ahmed Ould El Moctar, Franck Schoefs

► **To cite this version:**

Ziad Maksassi, Bertrand Garnier, Ahmed Ould El Moctar, Franck Schoefs. Thermal characterization of biofouling around a dynamic submarine electrical cable. Congrès Français de Thermique 2021, Jun 2021, Belfort, France. hal-03257933

HAL Id: hal-03257933

<https://hal.science/hal-03257933>

Submitted on 18 Jun 2021

HAL is a multi-disciplinary open access archive for the deposit and dissemination of scientific research documents, whether they are published or not. The documents may come from teaching and research institutions in France or abroad, or from public or private research centers.

L'archive ouverte pluridisciplinaire **HAL**, est destinée au dépôt et à la diffusion de documents scientifiques de niveau recherche, publiés ou non, émanant des établissements d'enseignement et de recherche français ou étrangers, des laboratoires publics ou privés.



Distributed under a Creative Commons Attribution 4.0 International License

Thermal characterization of biofouling around a dynamic submarine electrical cable

Ziad MAKSASSI^{1,2}, Bertrand GARNIER¹, Ahmed OULD EL MOCTAR¹, Franck SCHOEFS²

¹Université de Nantes, CNRS, Laboratoire de thermique et énergie de Nantes, LTeN, UMR 6607
Rue Christian Pauc, 44306 Nantes, France

²Université de Nantes, Institut de Recherche en Génie Civil et Mécanique, GeM, UMR CNRS 6183
Rue de la Noë, 44321 Nantes, France

*(Corresponding author: ziad.maksassi@univ-nantes.fr)

Abstract – The electric insulation system of high voltage dynamic cable is designed to support continuously a maximum conductor temperature of 90°C. However, the growth of biofouling, particularly mussels can modify the heat transfer around the cable. In our work we estimate the effective thermal conductivity of different types of mussels as well as the heat transfer coefficient of water around the mussels. The results showed that the effective thermal conductivity of juvenile mussels is lower than the effective thermal conductivity of adult mussels.

Keywords: Electric dynamic cable; Biofouling; Thermal analysis; Thermal characterisation of biofouling; Marine renewable energy.

Nomenclature

k_{biof}	mussels thermal conductivity, $W.m^{-1}.K^{-1}$	ρ	mass density, $kg.m^{-3}$
L	length of the tube, m	u	fluid velocity, $m.s^{-1}$
r_e	radius of external layer of mussels, m	Q	volumic power, $W.m^{-3}$
r_i	radius of internal layer of mussels, m	N	number of thermocouples
h_w	heat transfer coefficient of the water around the mussels, $W.m^{-2}.K^{-1}$	J	summation of the subtraction between numerical and measured temperatures
U	voltage, V	I	intensity, A
T	absolute temperature, K		

1. Introduction

Floating offshore wind turbine (FOWT) is one of leading developed renewable energy and is considered as a one of the main solutions against the effective warming. It's more efficient than the bottom-fixed offshore wind turbine and on land wind turbine since the speed of wind far from the coast is higher than the speed near the coast where a small increase in wind yields a large increase in energy production. For example, a turbine with 24 km/h wind can generates twice as much energy as a turbine with 19 km/h [1]. The advantages of installing FOWT over fixed-offshore wind farm are less visual disturbance, noise avoidance, stronger and more consistent wind, ability for installation in deep water, cheaper installation cost, no wind turbine size restrictions, easing to repair and last advantage is that the FOWT is more friendly to environment. On the contrary there are some disadvantages of FOWT like technical challenges for optimization of mooring lines and the electrical connection. In addition, shore-offshore distance makes the repair and maintenance operation more time consuming, therefore, costlier [2]. Electrical connection is one of the main challenge of floating offshore wind turbine, firstly the floating offshore wind turbine sends its power through dynamic power cable undersea to transformer then the transformer sends its power through static power cable to a converter platform. The alternating current is converted to a high direct current and is sent to a converter

station on land which transforms the power into three phases electric power. So, there are two categories of submarine power cable, the first category is called static cable which comes on top of or buried within the seafloor and the second category is called the dynamic cable (or umbilical) which are deployed through the water column between the surface and the seafloor as shown in figure 1.

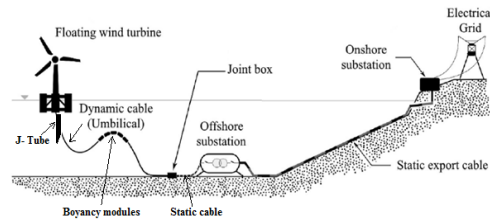


Figure 1: Power transmission system of floating offshore wind turbine[3]

Thus, the dynamic power cable is a main component in the electrical connection, its design is still a challenge to manufacturers, therefore, any external effect decreasing its efficiency will lead to receive less energy. Growth of biofouling, especially mussels can modified the heat transfer around the cable which could lead to decrease or increase the temperature of the cable, whereas as per IEC standard [4] the cross-linked polyethylene (XLPE) electric insulation system of high voltage dynamic cable (HVDC) is designed to support continuously a maximum copper wire temperature of only 90 °C. Thus, it's important to characterize the thermal effect of mussels around the cable in order to know if it will affect the heat transfer between cable and water in a positive or negative way, however, to do that a thermal characterization of mussels should be performed. To our knowledge, no prior studies exist about the thermal characterization of the mussels around the cable. In this work, the "effective" thermal conductivity of different types of mussels (juveniles, mixed (juveniles and adults) and adults, as shown in figure 2a, 2b and 2c respectively), is measured, as well as the heat transfer coefficient of water around the mussels. One should note that these mussels were extracted from the Atlantic Ocean on a mussel breeding site (Aiguillon sur Mer, France, July 8th 2020). Thermal properties measurement on mussel biofoulings were all performed within 24h after their withdraw from the sea in order to keep the mussels alive. The short time available for preparing the samples and performing all the steady state measurements was a strong constraint during the measurement campaign.



Figure 2: Different types of mussels: a) Juvenile, b) mix(juvenile and adult) and c) adult.

2. Methodology

The effective thermal conductivity of the mussels is computed using 1D analytical stationary model (Fourier's law) valid for an uniform distribution of the mussels around the tube. The measurement method is validated by measuring also the thermal conductivity of a double sided foam adhesive and by comparison with a measurement from a hot guarded plate device. In addition, the heat transfer coefficient of the water around the mussels is also computed using Newton's law. Also, it's compared with two correlations from the literature (Churchill & Chu

and Morgan [5]). Moreover, one have also considered non uniform distributions of mussels around the tube indeed in practice mussels growth occurs undersea mainly on the top of horizontal electric cable since the light is coming from above. In this case, due to more complicated geometry, the effective thermal conductivity of different types of mussels and heat transfer coefficient of the water around the mussels are estimated using numerical method (finite elements via COMSOL) to solve the 2D heat transfer equation and a parameter estimation technique (simplex method) is used to obtain the effective thermal conductivity of the mussels and the heat transfer coefficient of the water around the mussels.

2.1. Experimental setup

An experimental tube is used to perform the stationary measurements. It consists of an aluminum tube ($\phi_{int}=60\text{mm}$, $\phi_{ext}=65\text{mm}$, $L=600\text{mm}$) implemented with 5 K-type thermocouples (3 in the middle cross section with 120° angle and one thermocouple on two other cross-sections close to the extremities of the tube (at 5 cm). Six silicon rubber tapes ($L=600\text{ cm}$, $w=25.4\text{mm}$) with copper etched foil (SRFGA-124/2-P from Omega) are implemented on the inner side of the aluminum tube to provide a uniform heating. The 6 heaters are maintained in contact with the aluminum tube using a rubber air chamber with an internal pressure about 1,5 bar. Moreover, a sample holder is manufactured in order to allow the measurement inside a tank filled with sea water immobile. The supporting system for the aluminum tube consists of a POM (polyoxymethylene) seal fixed on each extremities of the tube using a plastic screw, carried up by a U-clamp connected to T-shape support, as shown in figure 3a. Then, the mussels are spreaded around the experimental tube and maintained using a steel net (1 cm mesh) as shown in figure 3b.

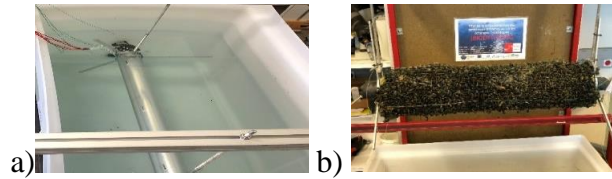


Figure 3: *Experimental tube a)without mussels b) with mussels.*

2.2. Measurement of the effective thermal conductivity and heat transfer coefficient

2.2.1. Analytical method (Fourier's law) for a uniform colonization around the tube

Fourier's law is used to calculate the effective thermal conductivity of mussels in case of uniform colonization (100 % coverage of mussels) and this using temperature discrepancy between the two sides of the mussel layer and the power crossing it. During the experiment, the tube is immersed in a tank filled with sea water and a power provided by the heating elements inside the tube is used to reach a steady state temperature with an increase about 5°C . Therefore, the computation of the effective thermal conductivity of mussels (k_{biof}) and of the heat transfer coefficient of water (h_w) around the mussels for an uniform colonization as shown in figure 4, is represented by the following equations (1) and (2), respectively:

$$k_{biof}(W.m^{-1}.K^{-1}) = \frac{\ln\left(\frac{r_e}{r_i}\right)*Q}{2\pi*L*(T_{av1}-T_{av2})} \quad (1)$$

$$h_w(W.m^{-2}.K^{-1}) = \frac{Q}{2\pi*r_e*L*(T_{av2}-T_w)} \quad (2)$$

where T_{av1} is the average temperature on the internal side of the mussel layer (average of T_1 , T_2 and T_3) measured by the three thermocouples in the middle cross-section and located in the

aluminum tube. T_{av2} is the average temperature on the external side of the mussel layer (average of T_4 , T_5 and T_6) and T_w is the temperature of the water far away from the aluminum tube.

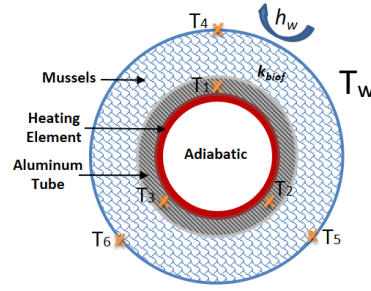


Figure 4: Middle cross-section of the aluminum tube covered with uniform colonization.

With noting that in accordance to the law of the propagation of uncertainties [5], the absolute uncertainty of the effective thermal conductivity of mussels is obtained by:

$$\delta k = \sqrt{\left(\frac{dk}{dL} \delta L\right)^2 + \left(\frac{dk}{dT_{av1}} \delta T_{av1}\right)^2 + \left(\frac{dk}{dT_{av2}} \delta T_{av2}\right)^2 + \left(\frac{dk}{dU} \delta U\right)^2 + \left(\frac{dk}{dI} \delta I\right)^2 + \left(\frac{dk}{dr_i} \delta r_i\right)^2 + \left(\frac{dk}{dr_e} \delta r_e\right)^2} \quad (3)$$

It follows then:

$$\delta k = \sqrt{\left(\frac{-\ln\left(\frac{r_e}{r_i}\right) * U * I}{2\pi L^2 (T_{av2} - T_{av1})} \delta L\right)^2 + \left(\frac{\ln\left(\frac{r_e}{r_i}\right) * U * I}{2\pi L (T_{av2} - T_{av1})^2} \delta T_{av1}\right)^2 + \left(\frac{-\ln\left(\frac{r_e}{r_i}\right) * U * I}{2\pi L (T_{av2} - T_{av1})^2} \delta T_{av2}\right)^2 + \left(\frac{\ln\left(\frac{r_e}{r_i}\right) * I}{2\pi L (T_{av2} - T_{av1})} \delta U\right)^2 + \left(\frac{\ln\left(\frac{r_e}{r_i}\right) * U}{2\pi L (T_{av2} - T_{av1})} \delta I\right)^2 + \left(\frac{-U * I}{2\pi L r_i (T_{av2} - T_{av1})} \delta r_i\right)^2 + \left(\frac{U * I}{2\pi L r_e (T_{av2} - T_{av1})} \delta r_e\right)^2} \quad (4)$$

Also, the uncertainties on the heat transfer coefficient h_w is calculated similarly as the one of thermal conductivity.

2.2.2. Numerical model (finite elements) and parameter estimation for a uniform colonization of biofouling around the tube

In this section the effective thermal conductivity of the mussels and the heat transfer coefficient of the water around the mussels are estimated using a 2D steady state thermal model computed using finite elements (COMSOL software) with the following heat conduction equation as shown in equation (5):

$$\text{div}(-k\nabla T) = Q \quad (5)$$

To solve equation (5), one has used a mesh with 2000 to 5000 nodes in the biofouling region and 1000 in the aluminum tube one. To estimate the effective thermal conductivity of mussels, a robust minimization technique is used (simplex method), in order to minimize the sum of square of the difference between measured and calculated temperatures, the latter depending on the three parameters values k_{biof} , h_{w1} and h_{w2} :

$$J = \sum_{i=1}^N (T_{i,calc.}(k_{biof}, h_{w1}, h_{w2}) - T_{i,meas.})^2 \quad (6)$$

Three different configurations of the distribution of the biofouling around the tube were considered as shown in figure 5.

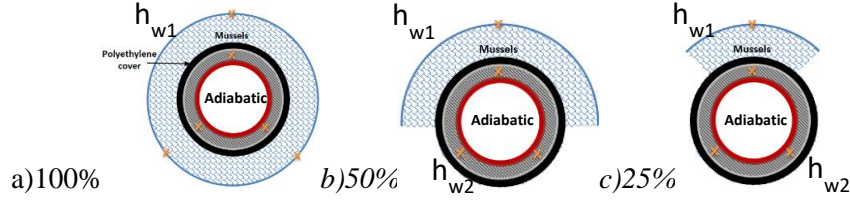


Figure 5: Different configurations of colonization distribution around the heated aluminum tube.

3. Results and discussion

3.1. Validation of the measurement method

The method and experimental setup designed to perform thermal characterization was tested using a material double sided tape adhesive which thermal conductivity was initially measured using a hot guarded plate (HGP) device with 5% relative uncertainty. The result shows that the thermal conductivity computed using equation (1) and our experimental setup with aluminum tube was equal to $0.052 \text{ W.m}^{-1}.\text{K}^{-1}$ (for double sided tape adhesive not covered with steel net) and $0.053 \text{ W.m}^{-1}.\text{K}^{-1}$ (for double sided tape adhesive covered with steel net) whereas the one with the HGP device was equal to $0.055 \text{ W.m}^{-1}.\text{K}^{-1}$ therefore with only a 5.45% and 3.64% relative discrepancy, respectively. This validation confirms that the steel net does not have a crucial effect on the value of the thermal conductivity. Also, it confirms that the extremities of the tube linked to the sample holder is quite well thermally insulated. In other words, the axial heat flux along the aluminum tube is negligible compared to the radial one which justify the fact that the direction along the tube length is not taken into account in our thermal models (analytical or numerical).

3.2. Uniform colonization around the tube

Table 1 shows that the measured values of the effective thermal conductivity of juvenile, mix (juvenile and adult) and adult mussels are 4.4, 8, 12.8 $\text{W.m}^{-1}.\text{K}^{-1}$ respectively, for a uniform distribution of mussels around the aluminum tube. As the relative uncertainty on k_{biof} measurement is less than 9 %, the differences are pertinent. One explanation of these discrepancies can be the size of mussels which are increasing with their age (Fig.2). Indeed, due to the different mussel sizes, the porosities of the three biofouling materials are getting higher with the age of mussels. Therefore, one expects more naturel convection inside older biofouling showing therefore a higher effective thermal conductivity. In addition, the effective thermal conductivity occurring here is indeed higher than that of water. However, the resulting resistance must be compared with that of convection around the tube in the absence of mussels. In the current situation these two resistances are roughly of the same order. However, in the practical situation, the configuration changes in the sense that the composition of the deposit and its thickness change over time during successive seasons of growth of the mussels. In this case we can expect that the resistance linked to the deposit will eventually prevail and therefore would lead to a situation where the tube is more thermally insulated, which will induce overheating of the electric cable detrimental to its service life.

Mussels type	k_{biof}	Absolute uncertainty	Relative uncertainty
	$\text{W.m}^{-1}.\text{K}^{-1}$	$\text{W.m}^{-1}.\text{K}^{-1}$	%
Juvenile	4.4	± 0.4	9
Mix(juvenile and adult)	8.0	± 0.52	6.5
Adult	12.8	± 0.97	7.6

Table 1: Measured effective thermal conductivities of different types of mussels uniformly distributed around the aluminum tube.

Table 2 shows the measured heat transfer coefficients of 3395, 873, 2682 $\text{W}\cdot\text{m}^{-2}\cdot\text{K}^{-1}$ around the juvenile, mix (juvenile and adult) and adult mussels respectively, for a uniform distribution of mussels around the tube. However, the relative uncertainty reaches 19%-37%, this due to the fact that the position of the external thermocouple is not very accurate (± 5 mm) and to the temperature discrepancy between mussels external layer and water which is very small. Considering the relatively high value of the convective heat transfer its contribution in the overall thermal resistance, between the cable and the external water, is small comparing the to the one of the biofouling.

Mussels type	h_w	Absolute uncertainty	Relative uncertainty	ΔT	Absolute uncertainty	Relative uncertainty
	$\text{Wm}^{-2}\text{K}^{-1}$	$\text{Wm}^{-2}\text{K}^{-1}$	%	$^{\circ}\text{C}$	$^{\circ}\text{C}$	%
Juvenile	3395	± 1123	33	0.23	± 0.07	30
Mix (juvenile & adult)	873	± 164	19	0.4	± 0.07	17.5
Adult	2682	± 1003	37	0.2	± 0.07	35

* ΔT : is the difference between the temperature on the external side of the mussel layer and the temperature of the water.

Table 2: *Experimental value of the heat transfer coefficient of the water around the mussels.*

After the previous measurement, one has checked the effect of water circulation in the open pores of the biofouling on the effective thermal conductivity. For this purpose, one has used a cluster of glass beads implemented around the experimental tube and maintained using a steel net as shown in figure 6a. The measured porosity of glass medium is about 43% and its measured effective thermal conductivity was found equal to $2.4 \text{ W}\cdot\text{m}^{-1}\cdot\text{K}^{-1}$ which is higher than the thermal conductivity of water ($0.6 \text{ W}\cdot\text{m}^{-1}\cdot\text{K}^{-1}$) and of the glass ($1.1 \text{ W}\cdot\text{m}^{-1}\cdot\text{K}^{-1}$). This shows that there is a small circulation of water in the porous space which leads to higher effective thermal conductivity. Also, a test is performed after covering the glass medium with a polyethylene stretch film as shown in figure 6b. Then, the effective thermal conductivity of the glass beads medium drops slightly to $2.19 \text{ W}\cdot\text{m}^{-1}\cdot\text{K}^{-1}$ so the difference is not exceeding 9%. Subsequently, the external water doesn't have a great effect on the value of the effective thermal conductivity of the porous medium. Moreover, the homogeneous effective thermal conductivity of glass beads due to Maxwell expression [7] gives a value of $0.93 \text{ W}\cdot\text{m}^{-1}\cdot\text{K}^{-1}$ which is lower than the measured effective thermal conductivity of the glass medium $2.4 \text{ W}\cdot\text{m}^{-1}\cdot\text{K}^{-1}$, where it should be noted that the homogeneous thermal conductivity of Maxwell is valid for small porosities up to 25%, however as mentioned before the porosity of our glass medium is 43%. Therefore, the hypothesis of the small circulation of water in the porous space which leads to a higher effective thermal conductivity is more likely.

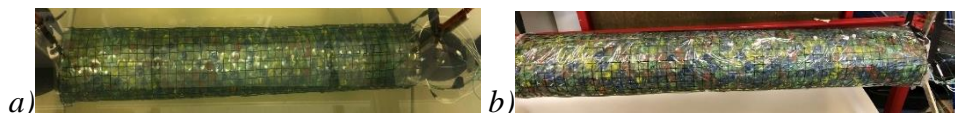


Figure 6: *Experimental tube covered with glass beads a) without plastic cover b) with plastic cover.*

Moreover, the analytical stationary method for the estimation of the heat transfer coefficient of the water around the mussels is validated by comparing the result of the heat transfer coefficient of the water around a tube without the presence of the mussels and two correlations from the literature (Churchill & Chu and Morgan [5]). Table 4 shows that the error between the experimental value and Morgan correlation is 6%, which is smaller than the error between the experimental and the Churchill & Chu correlation 29%, this due to the fact that in Churchill &

Chu correlation the Rayleigh number is considered for a wide range in contrast to the Morgan correlation. Moreover, it should be noted that the heat transfer coefficient obtained from the correlations is hiding all the complexity of the problem and all hypothesis are not quite well respected, thus the difference between the experimental and theoretical values obtained from correlations is acceptable.

h_w (<i>experimental</i>)	h_w (<i>Churchill & Chu</i>)	Error (<i>Experimental and Churchill & Chu</i>)	h_w (<i>Morgan</i>)	Error (<i>Experimental and Churchill & Chu</i>)
$\text{Wm}^{-2}\text{K}^{-1}$	$\text{Wm}^{-2}\text{K}^{-1}$	%	$\text{Wm}^{-2}\text{K}^{-1}$	%
220	309	29	234	6%

Table 4: *Experimental and theoretical values of the heat transfer coefficient of the water around the experimental tube without mussels.*

3.3. Non-uniform colonization around the tube

In real offshore installations, the mussels don't grow uniformly around the submarine cable. One reason for that is the non-uniform irradiation by the sun light. Thus, we are estimating the effective thermal conductivity of non-uniform mussels distribution around the tube and the heat transfer coefficient of the water around them. In the present simulation, the external temperature of the system is imposed as the temperature of the water and a power source is imposed by the heating elements. Table 5 shows the estimated effective thermal conductivity of juvenile mussels as well as the heat transfer coefficient of the water around the mussels with non-uniform colonization around the aluminum tube covered with polyethylene. One can note that there is a difference between the effective thermal conductivity of juvenile mussels for 100% colonization between the experimental aluminum tube with/without cover of polyethylene, this may be due to the fact that we don't have the same imposed heating flux and temperature gradient between the external layer and the internal layer of the mussels. That means that convection in the porous medium will not be the same and that will lead to different effective conductivities. Results in the table 5 shows that the effective thermal conductivity of uniform and non-uniform colonization has approximately the same order of magnitude, the difference can be related to the accuracy of the measurement and the temperature gradient between the external and the internal layer of mussels. It can be noted that the sensitivity of the heat transfer coefficient of the water around the mussels (h_{w1}) is small comparing to the sensitivity of the effective thermal conductivity. This result is coherent with our purely conductive model. A modification of this effective thermal conductivity is expected with the convection effect. Actually, in real application there is a current flow velocity of water in the system, then the effect of the global heat transfer coefficient of the water around the cable or mussels have to be considered. In our future work the right boundary conditions, taking the convection into account, will be considered through the simulation of the velocity distribution around the system.

Colonization %	k_{biof} $\text{W.m}^{-1}.\text{K}^{-1}$	Sensitivity $^{\circ}\text{C}$	h_{w1} $\text{W.m}^{-2}.\text{K}^{-1}$	Sensitivity $^{\circ}\text{C}$	h_{w2} $\text{W.m}^{-2}.\text{K}^{-1}$	Sensitivity $^{\circ}\text{C}$
25	1.4	1	1510	0.1	1960	0.9
50	1.9	1	310	0.1	3910	0.88
100	1.6	5	910	0.1	-	-

Table 5: *Effective thermal conductivity of juvenile mussels and heat transfer coefficient of water around the mussels for different % of colonization.*

4. Conclusion

In this work, one has performed the thermal characterization of mussels biocolonization. The experimental work is very challenging since we had to perform all the experiments within 24 hours to keep the mussels alive. The thermal conductivity of different types of mussels (juvenile, mix -juvenile and adult- and adult) as well as the heat transfer coefficient of the water around the mussels were estimated in the uniform mussels distribution case. We have obtained that juvenile mussels have the smallest effective thermal conductivity compared to the mix (juvenile and adult) and adult mussels respectively. This thermal characterization of the biofouling will allow in the future to compute the temperature distribution within the electric cable using an appropriate numerical model, knowing the structure of the cable and will help to predict the thermal contribution on the fatigue of those cables.

References

- [1] <https://www.americangeosciences.org/critical-issues/faq/what-are-advantages-and-disadvantages-offshore-wind-farms> (Available online : 5/5/2018).
- [2] R.Weerheim (2018). *Development of dynamic power cables for commercial floating wind farms*. Faculty of Mechanical, Maritime and Materials Engineering Department of Marine and Transport Technology. Delft University of Technology.
- [3] F. Adam, M.U.T Rentschler, P. Chainho, K. Krügel and P.C. Vicente. *Parametric study of dynamic inter-array cable systems for floating offshore wind turbines*. *Marine Systems & Ocean Technology*, 15 (2020) 16-25.
- [4] Calculation of the current rating, 2006,"Part 1-1 Current rating equations (100% load factor) and calculation of losses", IEC standard 60287-1-1.
- [5] F. P. Incropera, D.P. Dewitt, T.L. Bergman, A.S. Lavine. *Fundamentals of heat and mass transfer* (6th edition) (2007).
- [6] Moffat. *Describing the uncertainties in experimental results*. *Experimental thermal and fluid science*, 1(1):3–17, 1988.
- [7] Maxwell, J. C., *A Treatise on Electricity and Magnetism*, 3rd ed., Oxford University Press, Oxford, 1892.

Acknowledgements

This work was carried out within the framework of the WEAMEC, West Atlantic Marine Energy Community, and with funding from the Pays de la Loire Region. Also, I would like to thanks to Arnaud ARRIVE (Technician in LTeN) who helps in the fabrication of the experimental tube.